Persistent Na+ influx drives L-type channel resting Ca2+ entry in rat melanotrophs

Tomohiko Kayano, Yuto Sasaki, Naoki Kitamura, Nobuya Harayama, Taiki Moriya, G. Dayanithi, Alexei Verkhratsky, Izumi Shibuya

Persistent Na^+ influx drives L-type channel resting Ca^{2+} entry in rat melanotrophs

Tomohiko Kayano[1,2], Yuto Sasaki[1], Naoki Kitamura[1,2], Nobuya Harayama[3], Taiki Moriya [1,2], Govindan Dayanithi[4,5,6,7], Alexei Verkhratsky[8,9] and Izumi Shibuya[1,2]

[1] Laboratory of Veterinary Physiology, Joint Department of Veterinary Medicine, Faculty of Agriculture, Tottori University, Tottori, Japan
[2] The United Graduate School of Veterinary Science, Yamaguchi University, Yamaguchi, Japan
[3]Intensive Care Medicine, University Hospital, University of Occupational and Environmental Health, Kitakyushu, Japan
[4]Institut des Sciences Biologiques-Neurosciences, cognition, Centre National de la Recherche Scientifique, 3 rue Michel-Ange, Paris-France
[5]MMDN, Institut National de la Santé et de la Recherche Médicale U1198, Université Montpellier, Montpellier-France
[6]Ecole Pratique des Hautes Etudes-Sorbonne, Paris, France
[7]Department of Pharmacology and Toxicology, Faculty of Medicine, Charles University at Plzen, Plzen, Czech Republic.
[8]Faculty of Biology, Medicine and Health, University of Manchester, M13 9PT Manchester, UK
[9]Achucarro Centre for Neuroscience, IKERBASQUE, Basque Foundation for Science, 48011 Bilbao, Spain

Short Title: Ca^{2+} signals in rat melanotrophs

Numbers of figures and tables:7 figures and 1 table

Declarations of interest: none

Corresponding authors:
Prof. Dr. Izumi Shibuya, D.V.M., Ph.D.
Laboratory of Veterinary Physiology
Joint Department of Veterinary Medicine, Faculty of Agriculture
Tottori University, Tottori, 680-8553 Japan.
E-mail: ishibuya@muses.tottori-u.ac.jp
4-101, Koyama-cho Minami, Tottori, 680-8553, Japan
Tel: +81-857-31-5427; Fax: +81-857-31-5427

and

Prof. Dr. Govindan Dayanithi, M.Sc., Ph.D
MMDN, Institut National de la Santé et de la Recherche Médicale U1198
Université Montpellier
Place Eugene Bataillon
F-24095 Cedex 5-Montpellier
France
e.mail: gdaya@univ-montp2.fr
Tél : +33 4 67 14 33 86; Fax : +33 4 67 14 92 95

1. Introduction

Endocrine cells are electrically excitable, they generate action potentials (APs) that drive Ca^{2+} influx through plasmalemmal voltage-gated Ca^{2+} channels (VGCCs); resulting changes in the cytosolic Ca^{2+} concentration ($[Ca^{2+}]_i$) provide for stimulus-secretion coupling [1]. Majority of endocrine cells generate APs and secrete hormones spontaneously; in particular, anterior pituitary endocrine cells are known to be spontaneously active in the absence of stimulation [2-5]. The intermediate lobe of the rat pituitary gland consists of homogenous population of endocrine cells known as melanotrophs, which spontaneously secrete peptides derived from pro-opimelanocortin (POMC) including α-melanocyte-stimulating hormone (α-MSH) and β-endorphin [6-8]. This secretion is instigated by spontaneous AP firing, subsequent Ca^{2+} entry and Ca^{2+} signals that have been recorded *in situ* in rat pituitary slice [1, 9, 10]. This spontaneous activity and secretion are regulated by the secreto-inhibitory transmitters/modulators, such as dopamine [6, 11, 12] and PGE_2 [13, 14]. Freshly isolated and cultured melanotrophs express tetrodotoxin (TTX)-sensitive and TTX-resistant voltage-gated sodium channels (VGSCs) [15, 16]. Spontaneous AP firing has also been reported in rat pituitary slices; this firing lead to VGCC activation and $[Ca^{2+}]_i$ increase [9, 10]. However, inhibition of VGSCs by TTX affects neither hormone release [10, 15, 17] nor the resting membrane potential in a majority of pituitary cells [10, 18]. In rat melanotrophs, a typical resting potential lies around –35 mV [12] suggesting operation of depolarizing persistent current, of cationic or anionic nature in addition to a resting K^+ conductance. The activity of TTX-insensitive Na^+-conducting channels was suggested to contribute to the resting membrane potential and may account for the depolarization for endocrine cells in the pars distalis [19-21]. We tested the hypothesis that other channels such as hyperpolarization-activated/cyclic nucleotide-modulated (HCN) channel, Na^+ leak channel NALCN or transient receptor potential (TRP) channels, may potentially mediate resting Na^+ conductance in melanotrophs.

In pituitary cells, spontaneously active cation channels, presumably of the TRPC family, may contribute to the control of pacemaking depolarization [22]; similarly they may be

responsible for the background depolarizing conductance and triggering of APs in lactotrophs and GH_3 cells [23]. However, the regulatory mechanisms underlying resting Ca^{2+} entry of rat melanotrophs in unstimulated condition are unknown. In the present study we analyzed cellular mechanisms involved in Ca^{2+} homeostasis under resting conditions in primary cultures of rat melanotrophs using Fura-2 microfluorimetry and patch-clamp.

2. Materials and methods

2.1. Solutions and drugs

Unless otherwise stated, all standard chemicals were purchased from Sigma (St Louis, MO, USA). The solution containing reduced Na^+ was made by the isotonic replacement of Na^+ with N-methyl-D-glucamine$^+$ (NMDG) or LiCl (Wako Pure Chemical Industries, Osaka). Similarly, a solution with 60 mM K^+ solution was made by isotonic replacement of Na^+ by K^+. The nominally Ca^{2+}-free solution contained no added $CaCl_2$. Stock solutions of dopamine (0.1 mM), lidocaine (0.1 M), ruthenium red (10 mM), CsCl (1 M), ω-agatoxin IVA (0.1 mM), ω-conotoxin GVIA (1 mM) and SNX-482 (0.2 mM) (Peptide Institute, Country) and were dissolved in deionized H_2O; cyclopiazonic acid (CPA, 10 mM), nifedipine (1 mM, Wako Pure Chemical Industries, Osaka), nimodipine (10 mM), nicardipine (10 mM), capsazepine (10 mM), SB-366791 (10 mM), SKF-96365 (10 mM), RN-1734 (10 mM) and HC-067047 (10 mM), flufenamic acid (FFA, 100 mM) and 2,2-diphenyltetrahydrofuran (DPTHF, 10 mM) were dissolved in DMSO; and TTX (1 mM, Nacalai Tesque, Kyoto, Japan) was dissolved in a citrate-buffered solution; all stock solutions were stored at -30 ºC until use.

2.2. Cell dissociation

Male Wistar rats of 6 - 8 weeks (150 g – 200 g) were used. The animals were housed at 23 - 24˚C on a 12 h light (07h00 to 19h00), 12 h dark cycle. All experiments were carried out in accordance with the protocols of the Ethics Committee of Animal Care and Experimentation, Tottori University, and French European Communities Council Directive on animal experimentation and authorization.

Procedures for dissociation of rat melanotrophs have been described previously [13, 14]. In

brief, rats were sacrificed by the decapitation under the anesthesia with isoflurane. The pituitary neurointermediate lobe was isolated from the anterior lobe and transferred to a HEPES-buffered solution (HBS), comprising (in mM) 140 NaCl, 5 KCl, 2 $CaCl_2$, 1 $MgCl_2$, 10 HPEPS, 10 glucose (pH adjusted to 7.4 with NaOH), supplemented with 0.1% bovine serum albumin (BSA). The lobes were incubated in HBS, containing 0.2% trypsin type IV, at 37 ºC for 20 min with continuous shaking (100 cycles / min) and then incubated in HBS containing 0.002 % DNase and 0.2% trypsin inhibitor for 5 min. The lobes were the incubated in Ca^{2+}-free HBS containing 0.1% collagenase (Worthington Biochemicals, Lakewood, NJ, USA) for 15 min and triturated with a silicon-coated glass pipette. The isolated cells were suspended in Dulbecco's modified Eagle medium (DMEM, Gibco, Life Technologies, Carlsbad, CA, USA: Wako Pure Chemical Industries, Osaka, Japan) containing 4.5g/l of glucose and cultured on coverslips (11 mm in diameter, 0.12 mm thick) or on 22 mm in diameter, 0.17 mm thick glass-bottom dishes (WillCo Wells Dishes-BV, Amsterdam, Netherlands) coated with poly-D-lysine. The cells were kept 37 C in a humidified atmosphere of 95% air and 5% CO_2 and cultured until use. DMEM was supplemented with 10% fetal bovine serum (MP Biochemicals, Irvine, CA, USA), 100 U/ml of penicillin and 100 µg/ml of streptomycin. The experiments were performed after 24-48h in cultures.

2.3. Intracellular $[Ca^{2+}]_i$ measurements

The $[Ca^{2+}]_i$ in dissociated cells was measured with the fluorescent Ca^{2+} indicator, fura-2, according to procedures reported previously [24, 25]. In brief, the cells attached to round coverslips (11 mm in diameter) were incubated in HBS containing Fura-2/AM (3 µM, Merck, Whitehouse Station, NJ, U.S.A.) for 60 min at room temperature (22-24 ºC). After the incubation, a coverslip was mounted in a chamber fixed on the stage of an inverted fluorescence microscope (IX71, Olympus, Tokyo, Japan). Cells were continuously perfused with various experimental solutions through polyethylene tubes connected to a peristaltic pump (Minipuls 3, Gilson, Middleton, WI, USA) at a flow rate of 1.5 ml/min, which allows rapid (seconds) change of extracellular solution. Changes in $[Ca^{2+}]_i$ were measured by dual excitation microfluorometry using a digital image analyzer (Aqua Cosmos/Ratio, Hamamatsu Photonics, Hamamatsu, Japan). The fluorescence was

observed using a UV objective lens (UApo 20 X 3/340, Olympus), and the emission was monitored with a cooled CCD camera (ORCA-ER, Hamamatsu Photonics, Japan). Some $[Ca^{2+}]_i$ measurements were performed using a fluorescence microscope (AxioObserver.D1, Zeiss, Jena, Germany) equipped with an epifluorescence oil immersion objective (FLUAR 40X/1.3 oil and FLUOR 20X0.75, Zeiss, Jena, Germany). The fluorescence intensity was detected by using a cooled CCD camera (AxioCam MRm, Zeiss, Jena, Germany) and the whole system was controlled by Zeiss ZEN Imaging software (AxioVision Demo version) [26, 27]. The fluorescence was excited at 340 and 380 nm, and emission was measured at 510 nm. $[Ca^{2+}]_i$ values from these experiments were quantified with appropriate calibrations. In this system, the control and test solutions were applied using a multiple capillary perfusion system (200 µm inner diameter capillary tubing, flow rate 250 µl/min) and the cells were subjected to a constant fast flow control buffer.

2.4. Patch-clamp recordings

Melanotrophs were plated on coverslips (11 mm in diameter) and continuously perfused with HBS at a flow rate of 1 ml/min. The cell-attached and whole-cell recordings were made at room temperature (22-24 ºC). Recording pipettes were pulled from micro glass capillaries (GD-1.5, Narishige, Tokyo, Japan) by a framed puller (P-97, Sutter, Novato, CA, USA). The patch pipettes had the tip resistance of 2.5 to 4 MΩ. In the experiments to record currents in the cell-attached configurations and holding currents in the whole-cell configuration, pipettes were filled with the K-rich pipette solution consisting of (mM); 130 K^+-gluconate, 6 Na^+-gluconate, 0.9 $CaCl_2$, 4 $MgCl_2$, 10 EGTA, 10 HEPES, 2 ATP-Na_2 and 0.3 GTP (pH adjusted to 7.3 with Tris) or the Cs-rich pipette solutions consisting of (mM); 130 Cs-gluconate, 6 Na-gluconate, 0.9 $CaCl_2$, 4 $MgCl_2$, 10 EGTA, 10 HEPES, 2 ATP-Na_2 and 0.3 GTP (pH adjusted to 7.3 with Tris). The patch clamp amplifier used was EPC-10 (HEKA, Lambrecht, Pfalz, Germany). Currents were controlled and measured by Patch Master Software (HEKA) running on Macintosh (Apple, Cupertino, CA, USA). Stored data were analyzed off-line by IGOR Pro software (WaveMetrics, Lake Oswego, OR, USA). Data acquisition was performed at a sampling frequency of 1 kHz throughout the experiments by a personal computer (Macintosh, Apple) in conjunction with an analog-digital converter (Power Lab; AD Instruments, Castle Hill, NSW, Australia). Data

were analyzed with Patch Master (HEKA), Lab Chart (AD Instruments), IGOR Pro (Wavemetrics) and Excel (Microsoft, Redmond, WA, USA).

2.5. RT-PCR

Total RNA was extracted from tissues obtained from the intermediate lobes of the pituitary gland, using Trizol reagent (Life technologies, Carlsbad, California, USA) according to the manufacturer's protocol. Reverse transcription was performed with 1 μg total RNAs and an oligo dT primer using SuperScriptTM III Reverse Transcriptase (Life technologies) according to the manufacture's protocol. PCR was performed with 1 μl of first-strand cDNA, primer pairs listed in Table 1 and Emerald Amp MAX PCR Master Mix (Takara Bio Inc., Shiga, Japan). The PCR profiles was as follows: 94 °C for 30 s, 45 °C (TRPC) or 50 °C (TRPM and TPRV) for 30 s and 72 °C for 70 s, for 30 cycles. After amplification, PCR products and a 100 bp DNA ladder (Takara Bio) were electrophoresed with TAE buffer on 1.5% agarose gel (NIPPON GENE CO., LTD Tokyo, Japan) containing 1 μg/ml ethidium bromide. Bands were excited by ultraviolet light and photographed.

2.6. Statistics

Data are presented as mean values ± SEM (n = the number of observations). The statistical significance was assessed by Student's *t* test. Differences were considered statistically significant if $p < 0.05$.

3. Results

3.1. The source of Ca^{2+} setting resting $[Ca^{2+}]_i$

Melanotrophs, which responded to 30 s application of 60 mM K^+ with an increase in $[Ca^{2+}]_i$ by at least 30 nM and to a 2 min exposure to dopamine (1 μM) by a decrease of $[Ca^{2+}]_i$ larger than 10 nM, were considered healthy and were used for further analysis. Application of dopamine and removal of extracellular Ca^{2+} consistently caused significant reductions in resting $[Ca^{2+}]_i$. The mean $[Ca^{2+}]_i$ decrease was 41.6 ± 0.9 nM (n = 749) and 34.6 ± 3.3 nM (n = 28), respectively (Fig1.A (a), B). Application of 10 μM cyclopiazonic acid (CPA), an inhibitor of endoplasmic reticulum Ca^{2+}-ATPase did not alter the resting

$[Ca^{2+}]_i$ (Fig1. A (b)). In order to investigate which types of Ca^{2+} channels functionally contribute to maintain the resting $[Ca^{2+}]_i$, selective VGCC antagonists were used; these included nifedipine at 1 μM (Fig1. A (c)), nimodipine at 10 μM and nicardipine at 10 μM for the L-type channel; ω-agatoxin IVA at 100 nM for the P/Q-type; ω-conotoxin GVIA at 1 μM for the N-type and SNX-482 at 100 nM for the R-type channel. The effects of these blockers, Ca^{2+}-free, dopamine and CPA are summarized in Fig.1B. Application of L-type and N-type blockers decreased the resting $[Ca^{2+}]_i$: nifedipine, nimodipine and nicardipine reduced the resting $[Ca^{2+}]_i$ by 26.6 ± 1.1, 34.5 ± 3.6 and 32.1 ± 2.8 nM, respectively; whereas ω-Conotoxin GVIA reduced the resting $[Ca^{2+}]_i$ by 6.6 ± 4.3 nM. Both ω-agatoxin IVA and SNX-482 had no effects on the resting $[Ca^{2+}]_i$.

3.2 Dependence of $[Ca^{2+}]_i$ on extracellular Na^+ concentrations

Next, we examined the effects of the inhibitors of VGSC, TTX (1 μM) and lidocaine (1 mM); which both did not affect resting $[Ca^{2+}]_i$ (Fig. 2A (a, b)). In contrast, decreasing extracellular Na^+ concentration (replacement of Na^+ by $NMDG^+$) caused a rapid reduction in the resting $[Ca^{2+}]_i$ in a concentration-dependent manner (Fig. 2B). The amplitudes of the $[Ca^{2+}]_i$ decrease by lowering the extracellular Na^+ concentration to 100, 50 and 25 mM were 10.2 ± 1.3, 26.3 ± 2.4 and 36.8 ± 2.2 nM, respectively (Fig. 2C). However, replacement of extracellular Na^+ by Li^+ did not affect the resting $[Ca^{2+}]_i$.

In order to examine whether the extracellular Na^+ concentration contributes to the constitutive Na^+ conductance, the cells were clamped at –80 mV in the whole-cell configuration. While application of TTX, lidocaine and nifedipine had no effect on a holding current (data not shown), the reduction of the extracellular Na^+ concentration shifted the level of the holding current in positive direction in $[Na^+]_o$ concentration-dependent manner (Fig. 3A). The current densities at different $[Na^+]_o$ were: –8.7 ± 0.8 pA/pF at 145 mM; –7.1 ± 0.7 pA/pF at 100 mM, –5.5 ± 0.5 pA/pF at 50 mM and –4.6 ± 0.4 pA/pF at 25 mM Na^+ (Fig. 3B). After restoring $[Na^+]_o$ to 145 mM, the holding current shifted negatively (Fig. 3A). To examine whether the resting membrane potential was affected by the decrease in $[Na^+]_o$, we calculated the difference between the holding current in 145 mM Na^+ and in 25 mM Na^+ solutions when the pipette potential was

clamped at 0 mV in the cell-attached configuration. The holding current shifted positively at 25 mM $[Na^+]_o$ (Fig. 4A). A command pulse (5 mV, 50 ms) was applied every 10 s to calibrate currents to the change in the membrane potential (Fig. 4B). In addition, effects of $[Na^+]_o$ reduction on the basal levels of the membrane potential were examined in the current-clamp mode in the whole-cell configuration. Application of 25 mM Na^+ solution caused hyperpolarization (Fig. 4C). The amplitudes of the hyperpolarization of the membrane potential are summarized in Fig. 4D. These results indicate that the resting membrane potential of melanotrophs is regulated by a persistent Na^+ conductance.

When cells were clamped at –80 mV with the Cs^+-rich pipette solution, exposure to 25 mM Na^+ extracellular solution elicited a positive sift in the holding current. Addition of 300 µM Ba^{2+}, an inhibitor of inward rectifier K^+ channel (K_{ir}) or 5 mM tetraethylammonium (TEA), a voltage-gated K channel (K_v) inhibitor, to the 25 mM Na^+ solution did not change holding current. When the extracellular K^+ concentration was increased from 5 mM to 50 mM, the holding currents shifted negatively (almost to the basal level) (Fig. 5A). The current densities are shown in Fig. 5B. These results demonstrate that there is constitutively activated conductance not only for Na^+ and Li^+, but also for K^+ in rat melanotrophs.

3.3. Analyses of TRP-related molecules

Since it has been reported that activation of channels of the TRP superfamily leads to a depolarization of cells through Na^+ and Ca^{2+} influx (for review:[28]), we investigated the possible contribution of these channels to the resting $[Ca^{2+}]_i$ in rat melanotrophs. The RT-PCR of pituitary intermediate lobe tissues revealed expression of TRPV1 and TRPV4 mRNAs (Fig. 6B); with bands reflecting expression of TRPV1, TRPV1b and TRPV1_SON [24] subtypes. We also found mRNA for TRPC6 and TRPM3, 4, 5 (Fig. 6A, C). Subsequently we examined effects of the TRPV1 blockers, ruthenium red (RR) at 10 µM, capsazepine at 10 µM and SB-366791 at 10 µM, the TRPV3 blocker, DPTHF at 100 µM, the TRPV4 blockers, RN-1734 at 10 µM and HC-067047 at 10 µM and the TRPC blocker, SKF-96365 at 10 µM; we also tested the HCN blocker, Cs^+ at 1 mM. Among these, RR, capsazepine, RN-1734 and DPTHF significantly reduced the resting $[Ca^{2+}]_i$ by 6.1 ±

1.3 nM, 25.7 ± 2.8 nM, 7.2 ± 2.5 nM and 12.6 ± 2.7 nM, respectively. Other antagonists had little or no effect on the resting $[Ca^{2+}]_i$ (Fig. 7A). Furthermore, we examined effects of the blockers which caused a significant reduction in the resting $[Ca^{2+}]_i$ on ionic currents. The flufenamic acid (FFA, 100 μM), a blocker of nonselective cation channels and gadolinium (Gd^{3+}, 100 μM), a non-specific cation channel blocker were tested on the basal level of background currents, by clamping the voltage at –80 mV. Neither FFA nor Gd^{3+} significantly affected the holding current. RR had no effect on the holding current in whole-cell configuration when cells were clamped at 0 mV (Fig. 7B), which is the reversal potential of most cationic channels including TRP channels, but caused a positive shift of the holding current in voltage clamped at –80 mV (Fig 7C). The current densities reduced by each blocker are shown Fig. 7D. None of the blockers used here except RR significantly affected the holding current. Finally, dopamine (1 μM) had little or no effect on the holding current (the current densities before and during dopamine were -8.3 ± 3.2 pA/pF and -8.4 ± 3.1 pA/pF, n = 6).

4. Discussion

In the present study we identified a constitutively active cation conductance that maintains the resting potential of melanotrophs at the "window current" region for L-type VGCCs. This creates sustained Ca^{2+} influx, which was shown to be involved in the regulation of basal $[Ca^{2+}]_i$ and in the maintenance of the basal secretory response [6]. To our knowledge, this is the first characterization of the Na^+-permeable cation conductance constitutively active in rat melanotrophs.

Rat melanotrophs express five different Ca^{2+} channel types [13, 17, 29-31]. Our data show that the selective L-type VGCC antagonists and extracellular Ca^{2+} removal significantly reduced resting $[Ca^{2+}]_i$ in almost all rat melanotrophs. On the other hand, inhibition of endoplasmic reticulum Ca^{2+} accumulation did not affect resting $[Ca^{2+}]_i$ levels. These results are consistent with previous observations that the basal $[Ca^{2+}]_i$ in *Xenopus* melanotrophs is maintained by spontaneous Ca^{2+} entry without involving Ca^{2+} release from intracellular Ca^{2+} stores [32, 33].

In the rat melanotrophs, the P/Q-type VGCCs were shown to be the most abundant and they carry approximately a half of the total Ba^{2+} currents, whereas L- and R-type channels carried approximately one third and one fifth of those, respectively. The N-type channels currents contribute less than 10% of total Ca^{2+} current in rat melanotrophs [13]. Our pharmacological analysis revealed that the largest component of resting Ca^{2+} influx is mediated by L-type channels. One possible explanation for the larger contribution of L-type channels and the much smaller contribution of P/Q-type channels to the resting $[Ca^{2+}]_i$ compared to those to the total Ba^{2+} currents could be related to technical differences. It has been suggested that activation/inactivation states of VGCCs are under control by various factors including the phosphorylation/dephosphorylation states of the channel proteins [34]. The inactivation properties of VGCCs have been well documented: the half inactivation potential ($V_{1/2}$) of L-type channels ($Ca_v1.1$, $Ca_v1.2$, $Ca_v1.3$ and $Ca_v1.4$) are –7.7 mV [35], –1.7 mV [36], –33.5 mV [37] and –15.4 mV [38], respectively. The $V_{1/2}$ of N-type (Cav2.1), P/Q-type (Cav2.2) and R-type (Cav2.3) is –29.2 mV [39, 40], from –72.7 to –37.0 mV [41, 42] and –68.4 mV [43], respectively. Since it was also reported that the resting membrane potential in rat melanotrophs is around –35 mV [12], we assume that P/Q- and R-type channels are inactivated at resting membrane potential. It has been predicted that Ca^{2+} influx should be mediated by the high threshold L-type Ca^{2+} channels [12]. The subtype of L-type Ca^{2+} channels widely expressed in neuroendocrine cells has a significant window current at membrane potential close to -50 mM [44]. In the present study, we demonstrated (by using pharmacological approach) that L- type channels play an important role in maintaining the resting $[Ca^{2+}]_i$ in unstimulated condition. Although N-type VGCCs blockers caused some decrease of the resting $[Ca^{2+}]_i$ (even though the $[Ca^{2+}]_i$ reduction was much smaller than that caused by L-type blockers), the existence of N-type channels in rat melanotrophs remains controversial [11, 29, 30, 44-46], and postnatal down-regulation of N-type channels expression has been considered [13].

What sets the relatively positive resting membrane potential of melanotrophs? Isotonic replacement of Na^+ by large organic cation, $NMDG^+$, decreased both resting $[Ca^{2+}]_i$ and holding current; in the current-clamp it caused hyperpolarization. Replacement of extracellular Na^+ with Li^+ affects neither the resting $[Ca^{2+}]_i$ nor the holding current.

Decreasing Na^+ concentration caused a positive shift of the holding current, while in the presence of both K_{ir} and K_v channel blockers, increasing K^+ to 50 mM caused a negative shift of the holding current. These results suggest that rat melanotrophs possess constant conductance for Na^+, Li^+ and K^+.

Both GH_3 cells and rat somatotrophs express HCN channels [47-49] that play a key role in the control of neuronal rhythmicity ("pacemaker current") [50]. In addition, almost all endocrine cells express TRP channels, non-selective cation channels that are permeable to Ca^{2+} and Na^+ [51]. Among TRP channels, the TRPC family contributes to the background conductance and Ca^{2+} influx in lactotrophs, GH_3 cells [23] and anterior pituitary cells [22]. Since neither Cs^+, which blocks HCN channels, nor SKF96365, a selective TRPC channel blocker, altered $[Ca^{2+}]$i, we can exclude contribution of HCN and TRPC channels.

TRPV1-4 is thermosensitive nonselective cation channels [52, 53]. Nagata et al. [14] reported that the basal $[Ca^{2+}]_i$ ranged from 200 - 400 nM in rat melanotrophs at 35-37 ºC, which is similar to the values shown in other reports, i.e. 231 ± 23 nM at 32 ºC [54], 225 ± 3 nM at 37 ºC [55]; the resting $[Ca^{2+}]_i$ is somewhat lower at room temperature being measured at 160 ± 7 nM [12] and 162.0 ± 2.2 nM (present study). Although the difference could be due to the recording temperature, and/or the different methods for the $[Ca^{2+}]_i$ measurement with different calibration, these results may imply that the thermo-sensitive TRPV channels are possible candidates for persistent Na^+ conductance in rat melanotrophs. The RT-PCR analysis showed that the intermediate lobe tissue expresses TRPV1, TRPV4, TRPC6, TRPM3-5 channel mRNAs. Moreover, not only TRPV1, but also the two N-terminal splice variants of TRPV1, TRPV1a and TRPV1_SON [27] were expressed. Although our results do not exclude the possibility that these multiple TRP channels contribute to the resting $[Ca^{2+}]_i$ in melanotrophs, the lack of effects on the basal $[Ca^{2+}]_i$ and the holding current of the selective antagonists for TRPV4 and TRPC channels, as well as niflumic acid, which has been reported to have antagonist actions on TRPM channels [56] suggests that TRPV4, TRPC and TRPM channels may not play a role in rat melanotrophs. On the other hand, it should be noted that RR, a non-selective TRPV channel antagonist, demonstrated a marked positive shift of the holding current. RR also caused a significant

reduction in $[Ca^{2+}]_i$ thus supporting the role for TRPV1. The TPRV1 is known to pass Li^+ better than Na^+ [57], which also seems to match the results of the present study. Capsazepine, a TRPV1 antagonist, and DPTHF, a TRPV3 antagonist, caused a larger reduction in $[Ca^{2+}]_i$ than RR, however, had no effect on the holding current, suggesting that the effects on the basal $[Ca^{2+}]_i$ could reflect action on VGCCs. The lack of effects by capsazepine further suggests that the channel responsible for the cation conductance in rat melanotrophs is not a TRPV1 homotetramer. It has been reported that TRPV1 assemble either as homo- or heterotetramer to form cation channels, and that TRPV1 and TRPV2, and TRPV1 and VR.5′, another N-terminal splice variant of TRPV1, could co-assemble [58, 59]. It may be possible that in rat melanotrophs, TRPV1 heteromerizes with other members of the TRPV family including the two N-terminal splice variants of TRPV1 found in rat intermediate lobe in the present study, and such heteromerization could alter the pharmacology, which may explain the lack of effects of the TRPV1-specific drugs other than RR. Alternatively, unknown Na^+-permeating channels that are susceptible to the block by RR could be responsible for the persistent cation conductance. In any event, spontaneous Ca^{2+} entry associated with such cation conductance may play a stronger role in stimulus-secretion coupling of melanotrophs, as it has been reported that rat melanotrophs have smaller Ca^{2+}-buffering capacity than other secretory cells [54, 60].

Although dopamine via D_2 receptors potently suppresses $[Ca^{2+}]_i$ not only by directly inhibiting VGCCs, but also by activating GIRK channels to hyperpolarize and thereby deactivating Ca^{2+} channels [12, 14], it did not affect the holding currents in rat melanotrophs. Since the basal $[Ca^{2+}]_i$ in melanotrophs was shown to be maintained by spontaneous Ca^{2+} entry [6, 32, 33], it was obvious that a direct inhibition of VGCCs itself caused a reduction in $[Ca^{2+}]_i$. The finding that a reduction in extracellular Na^+ caused hyperpolarization implies that the decrease of $[Ca^{2+}]_i$ was due, at least in part, to the hyperpolarization-induced deactivation of VGCCs. Similar findings of nonselective conductance promoting Ca^{2+} entry through VGCCs and basal secretion are reported in lactotrophs [19] and in chromaffin cells [61, 62].

Taken together, our results demonstrated that rat melanotrophs possess a persistent cation conductance. The features of the cation channels clarified here are (i) permeable for Na^+, Li^+ and K^+, and (ii) sensitive to RR. Although further research is needed to clarify the molecular identity of the cation channels, the persistent Na^+ entry may play a direct and significant role in regulating $[Ca^{2+}]_i$ influx in unstimulated condition, which supplies Ca^{2+} to the sub-plasmalemmal site of exocytotic hormone release.

Conflicts of interest statement

The authors declare that there is no conflict of interest.

Acknowledgments

This study was supported by KAKENHI (Grant #:18380175, 25450464 and 16K08073) of Japan and the Japanese Society for Promotion of Science Fellowship Programs (#FY S-14191). G. Dayanithi belongs to the "Centre National de la Recherche Scientifique – The Ministry of Research and Higher Education-Paris", France.

References

[1] E.C. Toescu, G. Dayanithi, Neuroendocrine signalling: natural variations on a Ca^{2+} theme, Cell Calcium, 51 (2012) 207-211.
[2] P.S. Taraskevich, W.W. Douglas, Action potentials occur in cells of the normal anterior pituitary gland and are stimulated by the hypophysiotropic peptide thyrotropin-releasing hormone, Proc Natl Acad Sci U S A, 74 (1977) 4064-4067.
[3] P.S. Taraskevich, W.W. Douglas, Catecholamines of supposed inhibitory hypophysiotrophic function suppress action potentials in prolactin cells, Nature, 276 (1978) 832-834.
[4] P.S. Taraskevich, W.W. Douglas, Electrical behaviour in a line of anterior pituitary cells (GH cells) and the influence of the hypothalamic peptide, thyrotrophin releasing factor, Neuroscience, 5 (1980) 421-431.
[5] R. Zorec, S.K. Sikdar, W.T. Mason, Increased cytosolic calcium stimulates exocytosis in bovine lactotrophs. Direct evidence from changes in membrane capacitance, J Gen Physiol, 97 (1991) 473-497.
[6] W.W. Douglas, I. Shibuya, Calcium signals in melanotrophs and their relation to autonomous secretion and its modification by inhibitory and stimulatory ligands, Ann N Y Acad Sci, 680 (1993) 229-245.
[7] M. Rupnik, R. Zorec, Cytosolic chloride ions stimulate Ca^{2+}-induced exocytosis in melanotrophs, FEBS Lett, 303 (1992) 221-223.
[8] M. Rupnik, M. Kreft, S.K. Sikdar, S. Grilc, R. Romih, G. Zupancic, T.F. Martin, R. Zorec, Rapid regulated dense-core vesicle exocytosis requires the CAPS protein, Proc Natl Acad Sci U S A, 97 (2000) 5627-5632.
[9] S.S. Stojilkovic, H. Zemkova, F. Van Goor, Biophysical basis of pituitary cell type-specific Ca^{2+} signaling-secretion coupling, Trends Endocrinol Metab, 16 (2005) 152-159.
[10] S.S. Stojilkovic, J. Tabak, R. Bertram, Ion channels and signaling in the pituitary gland, Endocr Rev, 31 (2010) 845-915.
[11] D.M. Beatty, S.A. Sands, S.J. Morris, B.M. Chronwall, Types and activities of voltage-operated calcium channels change during development of rat pituitary neurointermediate lobe, Int J Dev Neurosci, 14 (1996) 597-612.
[12] A.K. Lee, Dopamine (D_2) receptor regulation of intracellular calcium and membrane capacitance changes in rat melanotrophs, J Physiol, 495 (Pt 3) (1996) 627-640.
[13] K. Tanaka, I. Shibuya, N. Kabashima, Y. Ueta, H. Yamashita, Inhibition of voltage-dependent calcium channels by prostaglandin E_2 in rat melanotrophs, Endocrinology, 139 (1998) 4801-4810.
[14] T. Nagata, N. Harayama, N. Sasaki, M. Inoue, K. Tanaka, Y. Toyohira, Y. Uezono, T. Maruyama, N. Yanagihara, Y. Ueta, I. Shibuya, Mechanisms of cytosolic Ca^{2+} suppression by prostaglandin E_2 receptors in rat melanotrophs, J Neuroendocrinol, 15 (2003) 33-41.
[15] S.J. Kehl, Voltage-clamp analysis of the voltage-gated sodium current of the rat pituitary melanotroph, Neurosci Lett, 165 (1994) 67-70.
[16] Y. Schwab, R. Jahke, E. Jover, Expression of tetrodotoxin-sensitive and resistant sodium channels by rat melanotrophs, Neuroreport, 15 (2004) 1219-1223.

[17] J. Stack, A. Surprenant, Dopamine actions on calcium currents, potassium currents and hormone release in rat melanotrophs, J Physiol, 439 (1991) 37-58.
[18] R. Kwiecien, C. Robert, R. Cannon, S. Vigues, A. Arnoux, C. Kordon, C. Hammond, Endogenous pacemaker activity of rat tumour somatotrophs, J Physiol, 508 (Pt 3) (1998) 883-905.
[19] S. Sankaranarayanan, S.M. Simasko, A role for a background sodium current in spontaneous action potentials and secretion from rat lactotrophs, Am J Physiol, 271 (1996) C1927-1934.
[20] M. Kucka, K. Kretschmannova, T. Murano, C.P. Wu, H. Zemkova, S.V. Ambudkar, S.S. Stojilkovic, Dependence of multidrug resistance protein-mediated cyclic nucleotide efflux on the background sodium conductance, Mol Pharmacol, 77 (2010) 270-279.
[21] P. Cobbett, C.D. Ingram, W.T. Mason, Sodium and potassium currents involved in action potential propagation in normal bovine lactotrophs, J Physiol, 392 (1987) 273-299.
[22] M. Tomić, M. Kucka, K. Kretschmannova, S. Li, M. Nesterova, C.A. Stratakis, S.S. Stojilkovic, Role of nonselective cation channels in spontaneous and protein kinase A-stimulated calcium signaling in pituitary cells, Am J Physiol Endocrinol Metab, 301 (2011) E370-379.
[23] M. Kučka, K. Kretschmannová, S.S. Stojilkovic, H. Zemková, M. Tomić, Dependence of spontaneous electrical activity and basal prolactin release on nonselective cation channels in pituitary lactotrophs, Physiol Res, 61 (2012) 267-275.
[24] T. Kayano, N. Kitamura, T. Moriya, A. Tsutsumi, Y. Ozaki, G. Dayanithi, I. Shibuya, Chronic treatment with NGF induces spontaneous fluctuations of intracellular Ca^{2+} in icilin-sensitive dorsal root ganglion neurons of the rat, J Vet Med Sci, 72 (2010) 1531-1538.
[25] Y. Ozaki, N. Kitamura, A. Tsutsumi, G. Dayanithi, I. Shibuya, NGF-induced hyperexcitability causes spontaneous fluctuations of intracellular Ca^{2+} in rat nociceptive dorsal root ganglion neurons, Cell Calcium, 45 (2009) 209-215.
[26] G. Dayanithi, O. Forostyak, Y. Ueta, A. Verkhratsky, E.C. Toescu, Segregation of calcium signalling mechanisms in magnocellular neurones and terminals, Cell Calcium, 51 (2012) 293-299.
[27] T. Moriya, R. Shibasaki, T. Kayano, N. Takebuchi, M. Ichimura, N. Kitamura, A. Asano, Y.Z. Hosaka, O. Forostyak, A. Verkhratsky, G. Dayanithi, I. Shibuya, Full-length transient receptor potential vanilloid 1 channels mediate calcium signals and possibly contribute to osmoreception in vasopressin neurones in the rat supraoptic nucleus, Cell Calcium, 57 (2015) 25-37.
[28] D.E. Clapham, D. Julius, C. Montell, G. Schultz, International Union of Pharmacology. XLIX. Nomenclature and structure-function relationships of transient receptor potential channels, Pharmacol Rev, 57 (2005) 427-450.
[29] J.A. Keja, J.C. Stoof, K.S. Kits, Dopamine D2 receptor stimulation differentially affects voltage-activated calcium channels in rat pituitary melanotropic cells, J Physiol, 450 (1992) 409-435.
[30] L. Ciranna, P. Feltz, R. Schlichter, Selective inhibition of high voltage-activated L-type and Q-type Ca^{2+} currents by serotonin in rat melanotrophs, J Physiol, 490 (Pt 3) (1996) 595-609.
[31] H.D. Mansvelder, J.C. Lodder, M.S. Sons, K.S. Kits, Dopamine modulates exocytosis independent of Ca^{2+} entry in melanotropic cells, J Neurophysiol, 87 (2002) 793-801.

[32] I. Shibuya, W.W. Douglas, Indications from Mn-quenching of Fura-2 fluorescence in melanotrophs that dopamine and baclofen close Ca channels that are spontaneously open but not those opened by high $[K^+]_O$; and that Cd preferentially blocks the latter, Cell Calcium, 14 (1993) 33-44.
[33] I. Shibuya, W.W. Douglas, Spontaneous cytosolic calcium pulses in Xenopus melanotrophs are due to calcium influx during phasic increases in the calcium permeability of the cell membrane, Endocrinology, 132 (1993) 2176-2183.
[34] I.B. Levitan, Modulation of ion channels by protein phosphorylation and dephosphorylation, Annu Rev Physiol, 56 (1994) 193-212.
[35] D. Freise, B. Held, U. Wissenbach, A. Pfeifer, C. Trost, N. Himmerkus, U. Schweig, M. Freichel, M. Biel, F. Hofmann, M. Hoth, V. Flockerzi, Absence of the gamma subunit of the skeletal muscle dihydropyridine receptor increases L-type Ca^{2+} currents and alters channel inactivation properties, J Biol Chem, 275 (2000) 14476-14481.
[36] P. Charnet, E. Bourinet, S.J. Dubel, T.P. Snutch, J. Nargeot, Calcium currents recorded from a neuronal alpha 1C L-type calcium channel in Xenopus oocytes, FEBS Lett, 344 (1994) 87-90.
[37] Y. Qu, G. Baroudi, Y. Yue, N. El-Sherif, M. Boutjdir, Localization and modulation of α1D (Cav1.3) L-type Ca channel by protein kinase A, Am J Physiol Heart Circ Physiol, 288 (2005) H2123-2130.
[38] L. Baumann, A. Gerstner, X. Zong, M. Biel, C. Wahl-Schott, Functional characterization of the L-type Ca^{2+} channel Cav1.4alpha1 from mouse retina, Invest Ophthalmol Vis Sci, 45 (2004) 708-713.
[39] E. Bourinet, T.W. Soong, K. Sutton, S. Slaymaker, E. Mathews, A. Monteil, G.W. Zamponi, J. Nargeot, T.P. Snutch, Splicing of alpha 1A subunit gene generates phenotypic variants of P- and Q-type calcium channels, Nat Neurosci, 2 (1999) 407-415.
[40] A. Stea, W.J. Tomlinson, T.W. Soong, E. Bourinet, S.J. Dubel, S.R. Vincent, T.P. Snutch, Localization and functional properties of a rat brain alpha 1A calcium channel reflect similarities to neuronal Q- and P-type channels, Proc Natl Acad Sci U S A, 91 (1994) 10576-10580.
[41] Z. Lin, Y. Lin, S. Schorge, J.Q. Pan, M. Beierlein, D. Lipscombe, Alternative splicing of a short cassette exon in alpha1B generates functionally distinct N-type calcium channels in central and peripheral neurons, J Neurosci, 19 (1999) 5322-5331.
[42] J.Q. Pan, D. Lipscombe, Alternative splicing in the cytoplasmic II-III loop of the N-type Ca channel alpha 1B subunit: functional differences are beta subunit-specific, J Neurosci, 20 (2000) 4769-4775.
[43] N.C. McNaughton, A.D. Randall, Electrophysiological properties of the human N-type Ca^{2+} channel: I. Channel gating in Ca^{2+}, Ba^{2+} and Sr^{2+} containing solutions, Neuropharmacology, 36 (1997) 895-915.
[44] J.C. Gomora, G. Avila, G. Cota, Ca^{2+} current expression in pituitary melanotrophs of neonatal rats and its regulation by D_2 dopamine receptors, J Physiol, 492 (Pt 3) (1996) 763-773.
[45] P.J. Williams, B.A. MacVicar, Q.J. Pittman, Synaptic modulation by dopamine of calcium currents in rat pars intermedia, J Neurosci, 10 (1990) 757-763.
[46] G. Cota, Calcium channel currents in pars intermedia cells of the rat pituitary gland. Kinetic properties and washout during intracellular dialysis, J Gen Physiol, 88 (1986) 83-105.

[47] K. Kretschmannova, A.E. Gonzalez-Iglesias, M. Tomić, S.S. Stojilkovic, Dependence of hyperpolarisation-activated cyclic nucleotide-gated channel activity on basal cyclic adenosine monophosphate production in spontaneously firing GH3 cells, J Neuroendocrinol, 18 (2006) 484-493.
[48] S.M. Simasko, S. Sankaranarayanan, Characterization of a hyperpolarization-activated cation current in rat pituitary cells, Am J Physiol, 272 (1997) E405-414.
[49] L. Tian, M.J. Shipston, Characterization of hyperpolarization-activated cation currents in mouse anterior pituitary, AtT20 D16:16 corticotropes, Endocrinology, 141 (2000) 2930-2937.
[50] C. Wahl-Schott, M. Biel, HCN channels: structure, cellular regulation and physiological function, Cell Mol Life Sci, 66 (2009) 470-494.
[51] J.A. Filosa, X. Yao, G. Rath, TRPV4 and the regulation of vascular tone, J Cardiovasc Pharmacol, 61 (2013) 113-119.
[52] C.D. Benham, M.J. Gunthorpe, J.B. Davis, TRPV channels as temperature sensors, Cell Calcium, 33 (2003) 479-487.
[53] S.F. Pedersen, G. Owsianik, B. Nilius, TRP channels: an overview, Cell Calcium, 38 (2005) 233-252.
[54] P. Thomas, A. Surprenant, W. Almers, Cytosolic Ca^{2+}, exocytosis, and endocytosis in single melanotrophs of the rat pituitary, Neuron, 5 (1990) 723-733.
[55] D.M. Beatty, B.M. Chronwall, D.E. Howard, T.B. Wiegmann, S.J. Morris, Calcium regulation of intracellular pH in pituitary intermediate lobe melanotropes, Endocrinology, 133 (1993) 972-984.
[56] G.L. Chen, B. Zeng, S. Eastmond, S.E. Elsenussi, A.N. Boa, S.Z. Xu, Pharmacological comparison of novel synthetic fenamate analogues with econazole and 2-APB on the inhibition of TRPM2 channels, Br J Pharmacol, 167 (2012) 1232-1243.
[57] A. Bouron, K. Kiselyov, J. Oberwinkler, Permeation, regulation and control of expression of TRP channels by trace metal ions, Pflugers Arch, 467 (2015) 1143-1164.
[58] H. Eilers, S.Y. Lee, C.W. Hau, A. Logvinova, M.A. Schumacher, The rat vanilloid receptor splice variant VR.5'sv blocks TRPV1 activation, Neuroreport, 18 (2007) 969-973.
[59] A.R. Rutter, Q.P. Ma, M. Leveridge, T.P. Bonnert, Heteromerization and colocalization of TrpV1 and TrpV2 in mammalian cell lines and rat dorsal root ganglia, Neuroreport, 16 (2005) 1735-1739.
[60] P.M. Lledo, P. Vernier, J.D. Vincent, W.T. Mason, R. Zorec, Inhibition of Rab3B expression attenuates Ca^{2+}-dependent exocytosis in rat anterior pituitary cells, Nature, 364 (1993) 540-544.
[61] T.R. Cheek, P. Thorn, A constitutively active nonselective cation conductance underlies resting Ca^{2+} influx and secretion in bovine adrenal chromaffin cells, Cell Calcium, 40 (2006) 309-318.
[62] M. O'Farrell, P.D. Marley, Different contributions of voltage-sensitive Ca^{2+} channels to histamine-induced catecholamine release and tyrosine hydroxylase activation in bovine adrenal chromaffin cells, Cell Calcium, 25 (1999) 209-217.
[63] X.R. Yang, M.J. Lin, L.S. McIntosh, J.S. Sham, Functional expression of transient receptor potential melastatin- and vanilloid-related channels in pulmonary arterial and aortic smooth muscle, Am J Physiol Lung Cell Mol Physiol, 290 (2006) L1267-1276.

[64] J. Wang, L.A. Shimoda, J.T. Sylvester, Capacitative calcium entry and TRPC channel proteins are expressed in rat distal pulmonary arterial smooth muscle, Am J Physiol Lung Cell Mol Physiol, 286 (2004) L848-858.

Figure legends

Figure 1. Contribution of voltage-gated Ca^{2+} channels (VGCCs) and intracellular Ca^{2+} stores to maintain of a resting $[Ca^{2+}]_i$ level.
(A) Representative trace showing $[Ca^{2+}]_i$ responses to dopamine and removal of extracellular Ca^{2+} (a), cyclopiazonic acid (CPA, b) and nifedipine (c). (B) Summary results of Ca^{2+} removal, CPA and the VGCC blockers on basal $[Ca^{2+}]_i$. Data are shown as the change of $[Ca^{2+}]_i$ caused by each manipulation. The values were calculated from difference between data for 2 min just before (Control) and data for 2 min before the finishing of each manipulation. The numbers of cells tested are shown in the figure. The vertical lines indicate SEM. *: $p<0.05$, **: $p<0.01$, ***: $p<0.001$ vs a basal $[Ca^{2+}]_i$ (Control), by paired T-test.

Figure 2. Effects of VGSC blockers and extracellular Na^+ reduction on maintenance of $[Ca^{2+}]_i$ level. (A) Representative $[Ca^{2+}]_i$ responses to TTX at 1μM (a, n = 32), lidocaine (Lid) at 1 mM (b, n = 24) and a decrease in extracellular Na^+ concentration from 145 mM to 100, 50 and 25 mM (B, n = 55). (C) Summary data for the effects of reduction of extracellular Na^+ concentration and VGSC blockers on a resting $[Ca^{2+}]_i$. Data are shown as the change of $[Ca^{2+}]_i$ ($\Delta[Ca^{2+}]_i$) caused by each manipulation. The numbers of cells tested are shown in the figure. The vertical lines indicate mean ± SEM. ***: $p<0.001$ vs basal $[Ca^{2+}]_i$ (Control), by paired T-test. †††: $p<0.001$, by T-test.

Figure 3. The holding current recorded under the voltage-clamp configuration is dependent on the extracellular Na^+ concentration.
(A) A typical trace of a holding current response to decreases of the extracellular Na^+ concentration to 100, 50, and 25 mM. The cells were voltage clamped at –80 mV. (B) Summary date for the current density recorded with the various extracellular Na^+ concentrations. The data are shown as the mean ± SEM (n = 9). ***: $p<0.001$, by paired T-test.

Figure 4. Effects of the extracellular Na^+ reduction on a resting membrane potential.
(A) A representative current trace recorded in the on-cell configuration in the presence of 25 mM extracellular Na^+ is shown. (B) Estimated change in the membrane potential from on-cell configuration is shown. Difference between the membrane potentials in the presence of decreased concentration of Na^+ and in the presence of 145-mM Na^+ was calculated. The vertical lines indicate SEM. (C) A typical trace of membrane potential under the current-clamp configurations is shown. (D) The change of the membrane potential by 25-mM Na^+ solution application in current-clamp configuration is indicated by the columns. The numbers of cells tested are shown in the figure. The vertical lines indicate SEM.

Figure 5. The resting current is permeable to K^+ and is not due to IRK and K_v channels.
(A) A holding current from melanotrophs voltage-clamped at –80 mV. The reduction of extracellular Na^+ concentration to 25 mM shifted a holding current positively in the absence and the presence of 300 μM Ba^{2+} and 5 mM TEA. Subsequently, increase of extracellular K^+ concentration to 50 mM negatively shifted a holding current that was shifted by application of 25 mM Na^+ solution in the presence of Ba^{2+} and TEA. (B) Quantitation of changes of holding current shown in (A). Data show a change of the holding current density with the absolute value (mean ± SEM, n = 6) for each manipulation. *: $p<0.05$, **: $p<0.01$, ***: $p<0.001$, by paired T-test.

Figure 6. RT-PCR analysis of mRNAs for TRPM2-5, TRPC3-7, TRPV2-4 and TRPV1-related molecules expressed in the intermediate lobe of the rat pituitary gland.
The total RNAs from the intermediate lobe were reverse transcribed, and amplified by PCR with each primer pair described in Table 1. Amplification products were electrophoresed on 1.5 % agarose gel and visualized by ethidium bromide. The expected size of the PCR products is indicated by arrowheads in the right side of each lane. Lane M, DNA marker. (A) Results of RT-PCR for *Trpc3, 4, 5, 6, 7*. (B) Results of RT-PCR for *Trpv2, 3, 4* and *Trpv1*-related molecules. (C) Results of RT-PCR for *Trpm2, 3, 4, 5*.

Figure 7. Effects of cation and TRP channel blockers on resting $[Ca^{2+}]_i$ level and a holding current in dissociated rat melanotrophs. (A) Summary results of effects of various blockers on resting $[Ca^{2+}]_i$ level. Data are shown as the change of $[Ca^{2+}]_i$ caused by each manipulation. The cells were treated by each manipulation for 3 min. The values are calculated from difference between data for 2 min just before (Control) and data for 2 min before the finishing of each manipulation. The numbers of cells tested are shown in the figure. A typical trace of a holding current response to an application of RR in the on-cell configurations voltage-clamped 0 mV (B) and whole–cell configurations voltage clamped at –80 mV. (C) Summary date for the current density recorded in the whole–cell configurations voltage clamped at –80 mV of each antagonist. The vertical lines indicate SEM. *: $p<0.05$, **: $p<0.01$, ***: $p<0.001$ vs basal, by paired T-test.

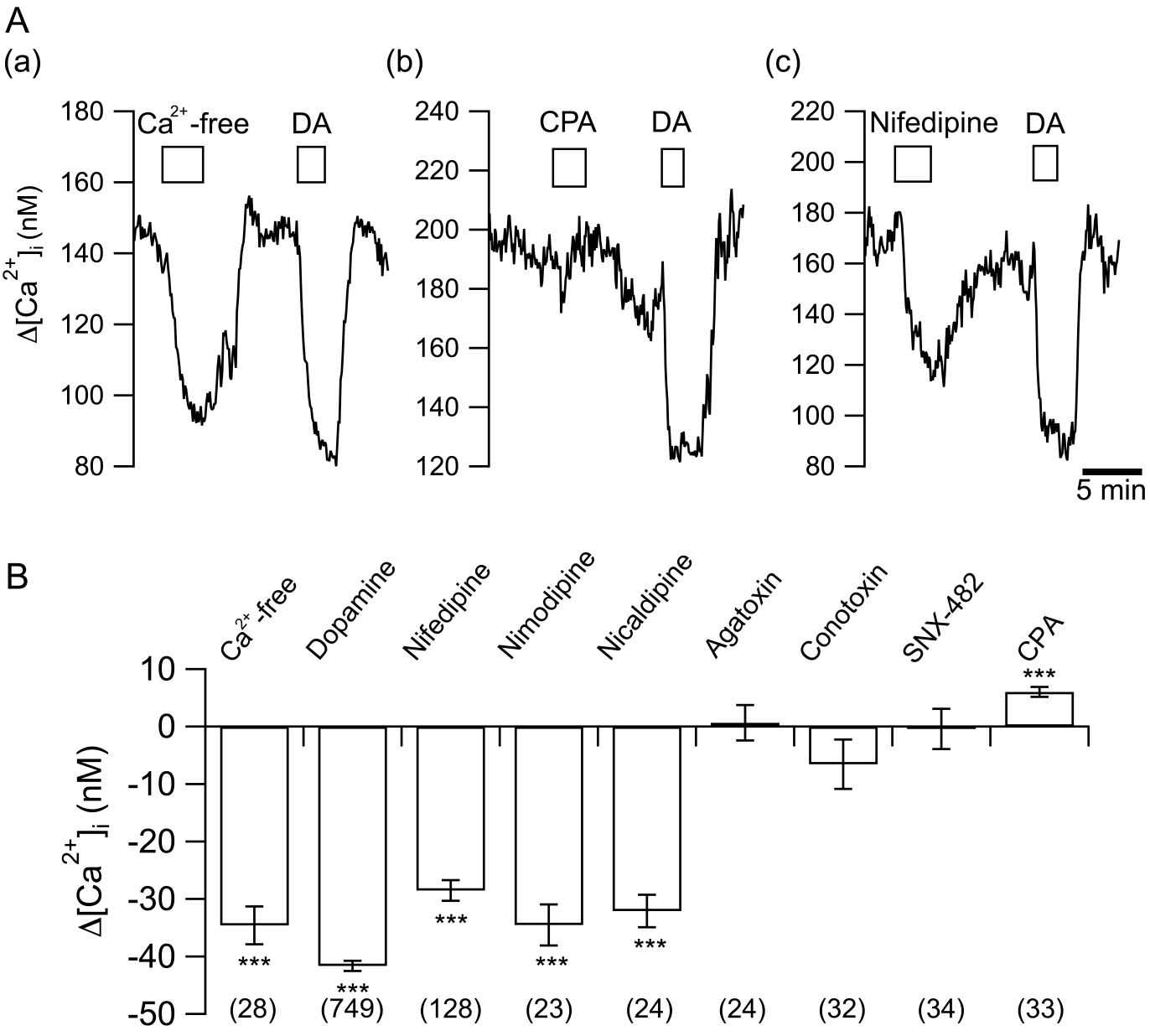
A
(a)
(b)
(c)
Ca2+-free
DA
CPA
DA
Nifedipine
DA
Δ[Ca2+]i (nM)
5 min
B
Ca2+-free
Dopamine
Nifedipine
Nimodipine
Nicaldipine
Agatoxin
Conotoxin
SNX-482
CPA
Δ[Ca2+]i (nM)
***
(28)
(749)
(128)
(23)
(24)
(24)
(32)
(34)
(33)

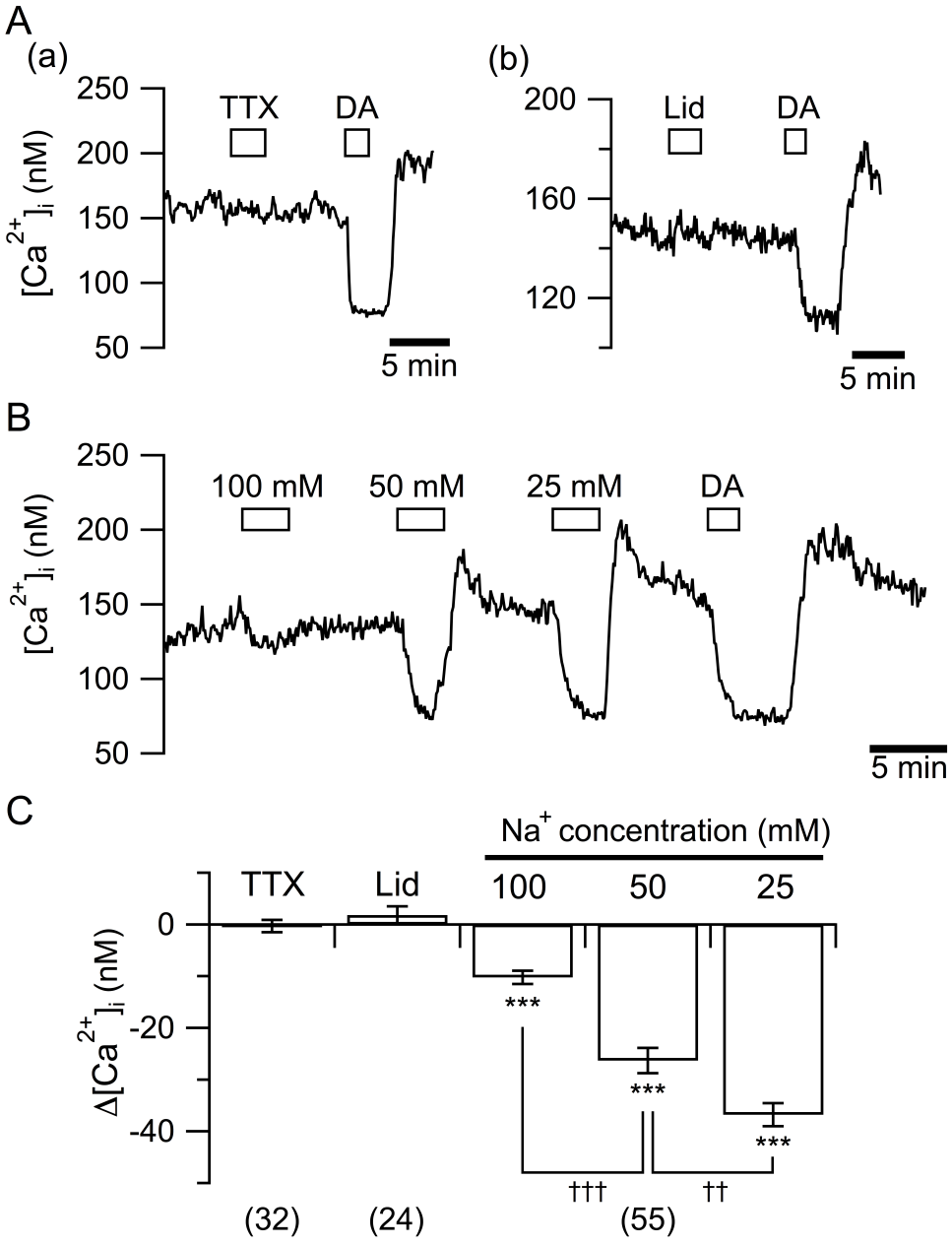
A
(a)
250
200
150
100
50
TTX
DA
5 min
(b)
200
160
120
Lid
DA
5 min
[Ca2+]i (nM)
B
250
200
150
100
50
100 mM
50 mM
25 mM
DA
5 min
[Ca2+]i (nM)
C
Na+ concentration (mM)
TTX
Lid
100
50
25
0
-20
-40
***
***
***
†††
††
(32)
(24)
(55)
Δ[Ca2+]i (nM)

Fig. 3

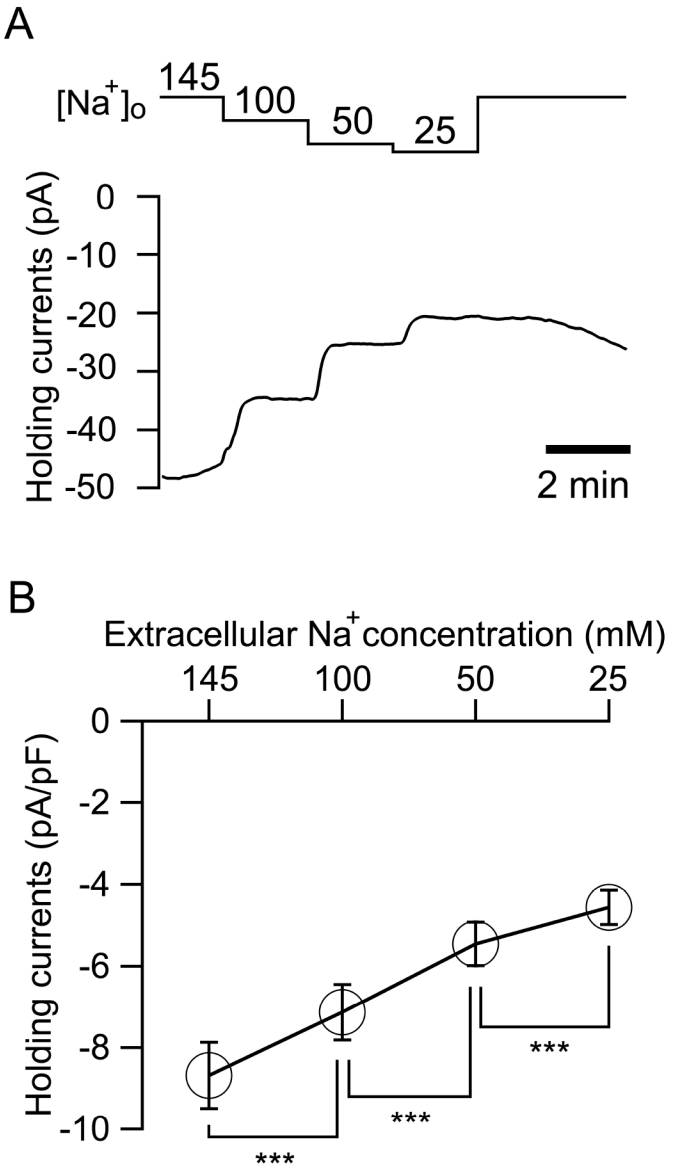
A
[Na+]o
145
100
50
25
Holding currents (pA)
0
-10
-20
-30
-40
-50
2 min
B
Extracellular Na+ concentration (mM)
145
100
50
25
Holding currents (pA/pF)
0
-2
-4
-6
-8
-10
***
***
***

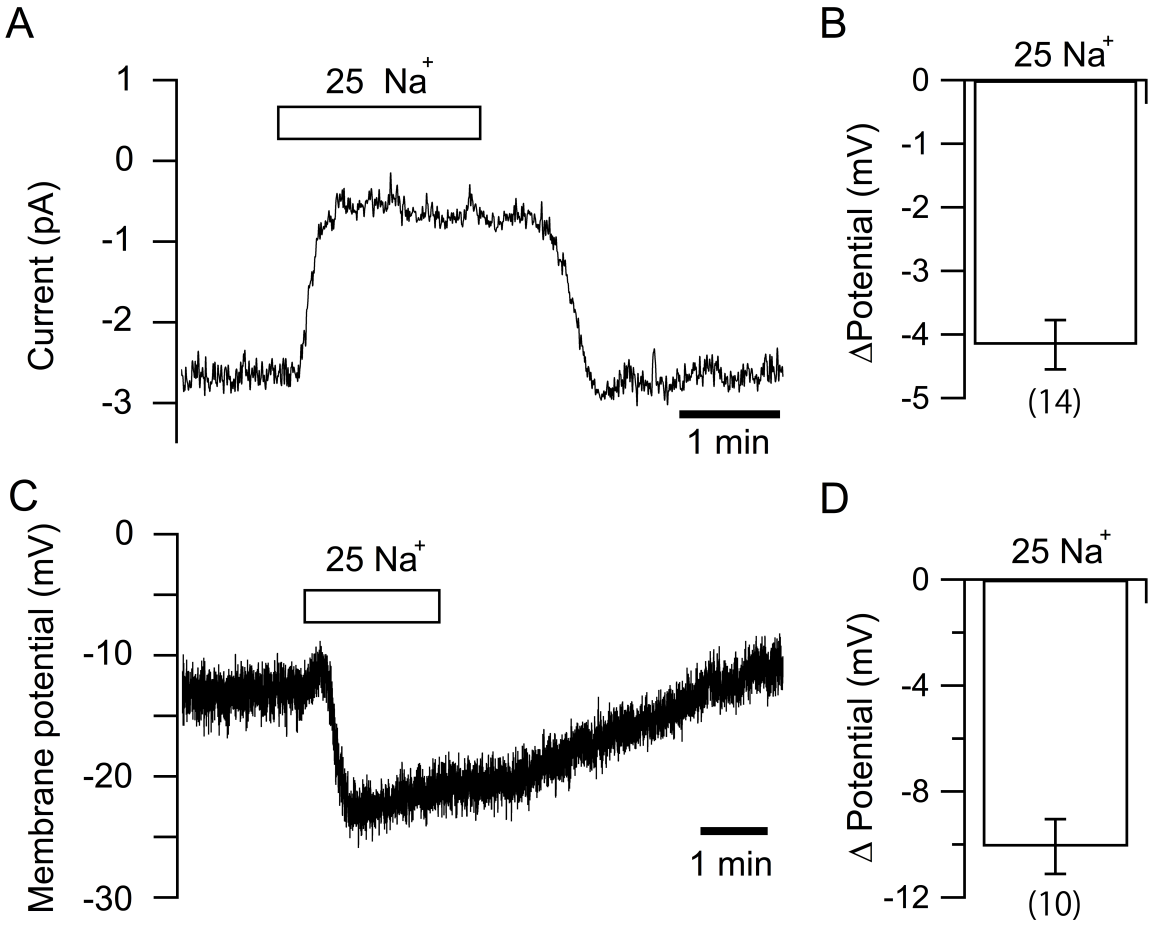
A
25 Na+
1
0
-1
-2
-3
Current (pA)
1 min
B
25 Na+
0
-1
-2
-3
-4
-5
ΔPotential (mV)
(14)
C
0
-10
-20
-30
Membrane potential (mV)
25 Na+
1 min
D
25 Na+
0
-4
-8
-12
Δ Potential (mV)
(10)

Fig. 5

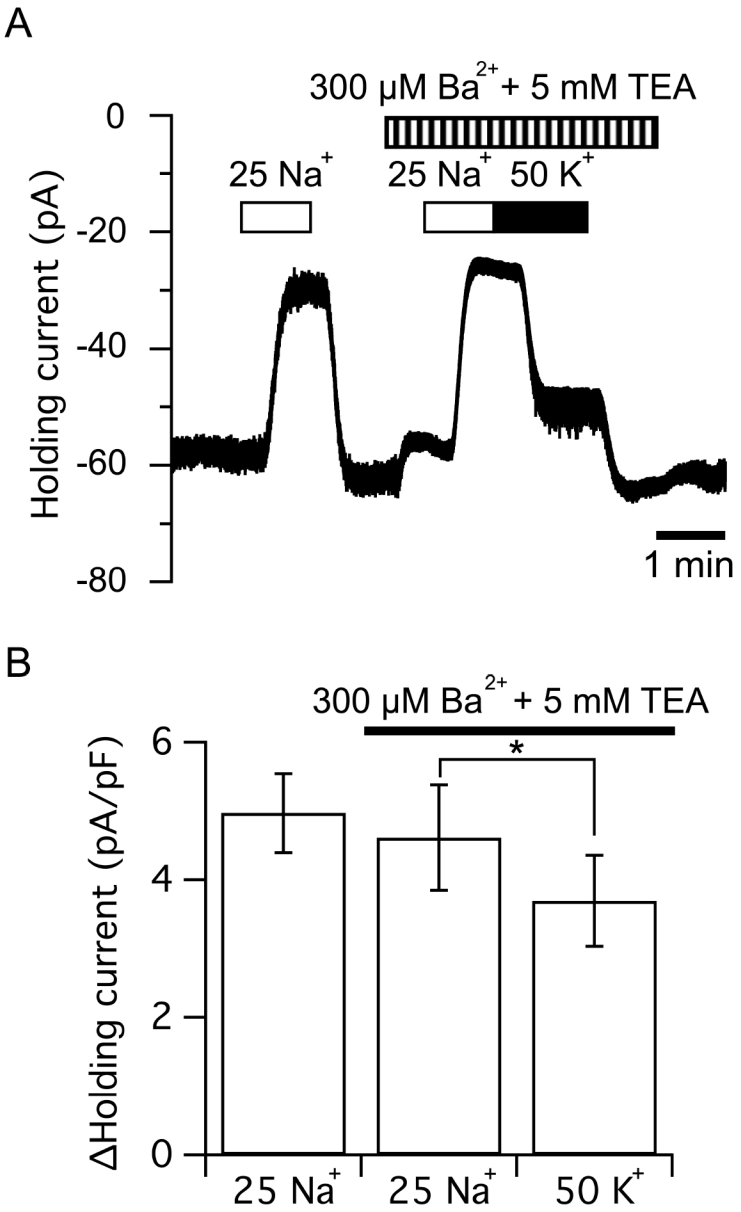
A
300 μM Ba2+ + 5 mM TEA
25 Na+
25 Na+ 50 K+
Holding current (pA)
0
-20
-40
-60
-80
1 min
B
300 μM Ba2+ + 5 mM TEA
*
ΔHolding current (pA/pF)
6
4
2
0
25 Na+
25 Na+
50 K+

Fig. 6

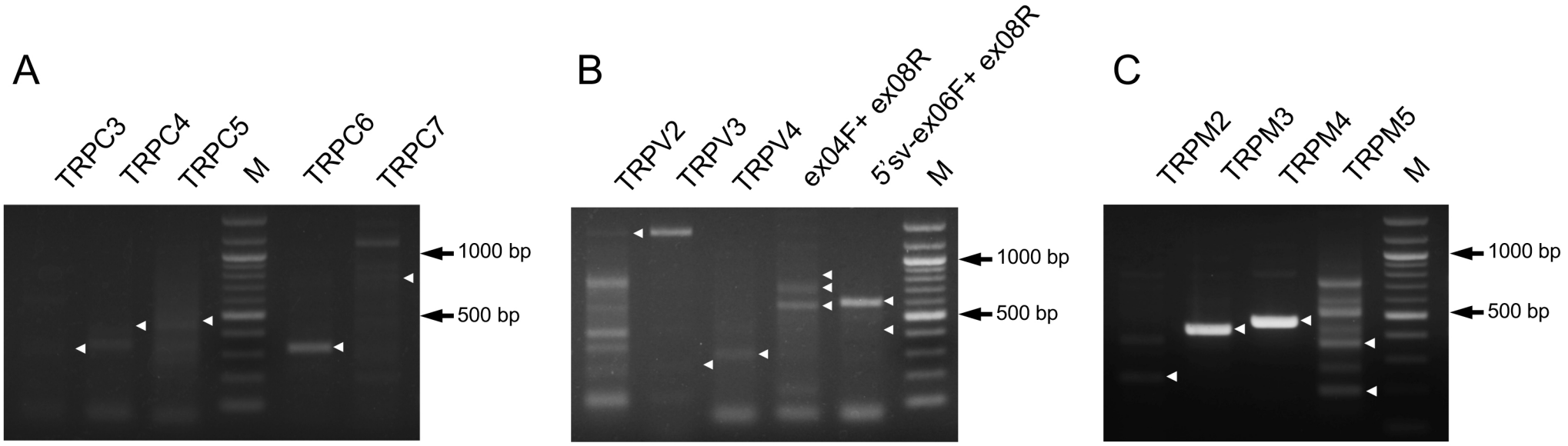
A
TRPC3
TRPC4
TRPC5
M
TRPC6
TRPC7
1000 bp
500 bp
B
TRPV2
TRPV3
TRPV4
ex04F+ ex08R
5'sv-ex06F+ ex08R
M
1000 bp
500 bp
C
TRPM2
TRPM3
TRPM4
TRPM5
M
1000 bp
500 bp

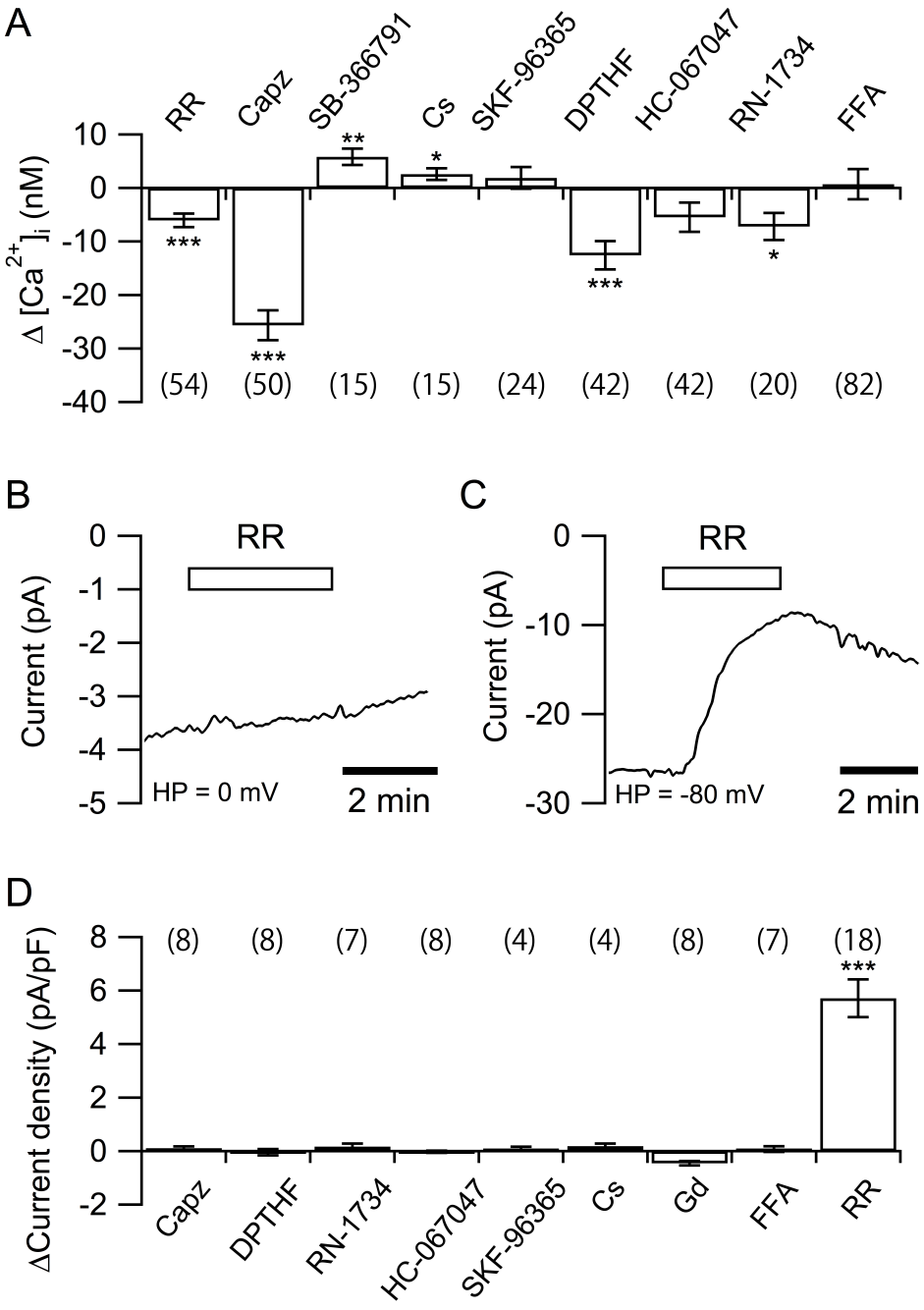
A
RR
Capz
SB-366791
Cs
SKF-96365
DPTHF
HC-067047
RN-1734
FFA
Δ [Ca2+]i (nM)
10
0
-10
-20
-30
-40
**
*
***
***
*
(54)
(50)
(15)
(15)
(24)
(42)
(42)
(20)
(82)
B
RR
Current (pA)
0
-1
-2
-3
-4
-5
HP = 0 mV
2 min
C
RR
Current (pA)
0
-10
-20
-30
HP = -80 mV
2 min
D
ΔCurrent density (pA/pF)
8
6
4
2
0
-2
(8)
(8)
(7)
(8)
(4)
(4)
(8)
(7)
(18)
***
Capz
DPTHF
RN-1734
HC-067047
SKF-96365
Cs
Gd
FFA
RR

Table 1. Primers for RT-PCR

Gene	Accession No.	Primer	Sequence (5'-3')	Product Size (bp)	Reference
Trpv1	NM_031982	ex04F	GACAGACAGCCTGAAGCAGT	740	[27]
		ex08R	ATCTGTCCCACTTGTCCTGT		
Trpv1b	AB041029	ex04F	GACAGACAGCCTGAAGCAGT	560	[27]
		ex08R	ATCTGTCCCACTTGTCCTGT		
Trpv1$_{var}$		ex04F	GACAGACAGCCTGAAGCAGT	841	[27]
		ex08R	ATCTGTCCCACTTGTCCTGT		
Trpv1_son	LC008303	5'SV-ex06F	CCAATCATCCAGGGACTAGC	605	[27]
		ex08R	ATCTGTCCCACTTGTCCTGT		
Vr.5'sv	AF158248	5'SV-ex06F	CCAATCATCCAGGGACTAGC	426	[27]
		ex08R	ATCTGTCCCACTTGTCCTGT		
Trpv1$_{var}$		5'SV-ex06F	CCAATCATCCAGGGACTAGC	605	[27]
		ex08R	ATCTGTCCCACTTGTCCTGT		
Trpv2	NM_017207	Forward	ACCGTGACCGACTCTTCAGT	1131	[63]
		Reverse	GCTGGCCCAGTAAGAGGTAA		
Trpv3	NM_001025757	Forward	ACGGTGGAGAACGTCTCC	240	[63]
		Reverse	TGTCCGTCTTATGGGCCC		
Trpv4	NM_023970	Forward	CCAACCTGTTTGAGGGAGAG	287	[63]
		Reverse	TGGCTGCTTCTCTACGACCT		
Trpc3	NM_021771	Forward	TGACTTCTGTTGTCCTCAAATATG	315	[64]
		Reverse	TCTGAAGTCTTCTCCTCCTGC		
Trpc4	NM_080396	Forward	TCTGCAGATATCTCTGGGAAGAATGC	415	[64]
		Reverse	AAGCTTTGTTCGAGCAAATTTCCACTC		
Trpc5	NM_080898	Forward	ACCTCTCATCAGAACCATGCCA	444	[64]
		Reverse	TGCATGAGCAAGTCACAGGCCT		
Trpc6	NM_053559	Forward	AAAGATATCTTCAAATTCATGGTC	323	[64]
		Reverse	CACATCCGCATCATCCTCAATTTC		
Trpc7	NM_001191691	Forward	TGTAACGCTGCACAACGTCTCA	767	[63]
		Reverse	AATTCCTCATGCCGGCCTGGTA		
Trpm2	NM_001011559	Forward	CTGATCAAGAGGAGGGCTTT	232	[63]

		Reverse	CACACTACCTTCCCTGCATC		
Trpm3	NM_001191562	Forward	GAGAGTGACCCGGATGAAAG	425	[63]
		Reverse	TTGAAGGTGTTCCCTTCCTG		
Trpm4	NM_001136229	Forward	GAGAGGATCATGACCCGAAA	463	[63]
		Reverse	GAACTTGCCCCACATTAGGA		
Trpm5	NM_001191896	Forward	CAGCAACACCTGGAGAGAGA	267	[63]
		Reverse	AGCCAGTGTGTCAGTCATGG		

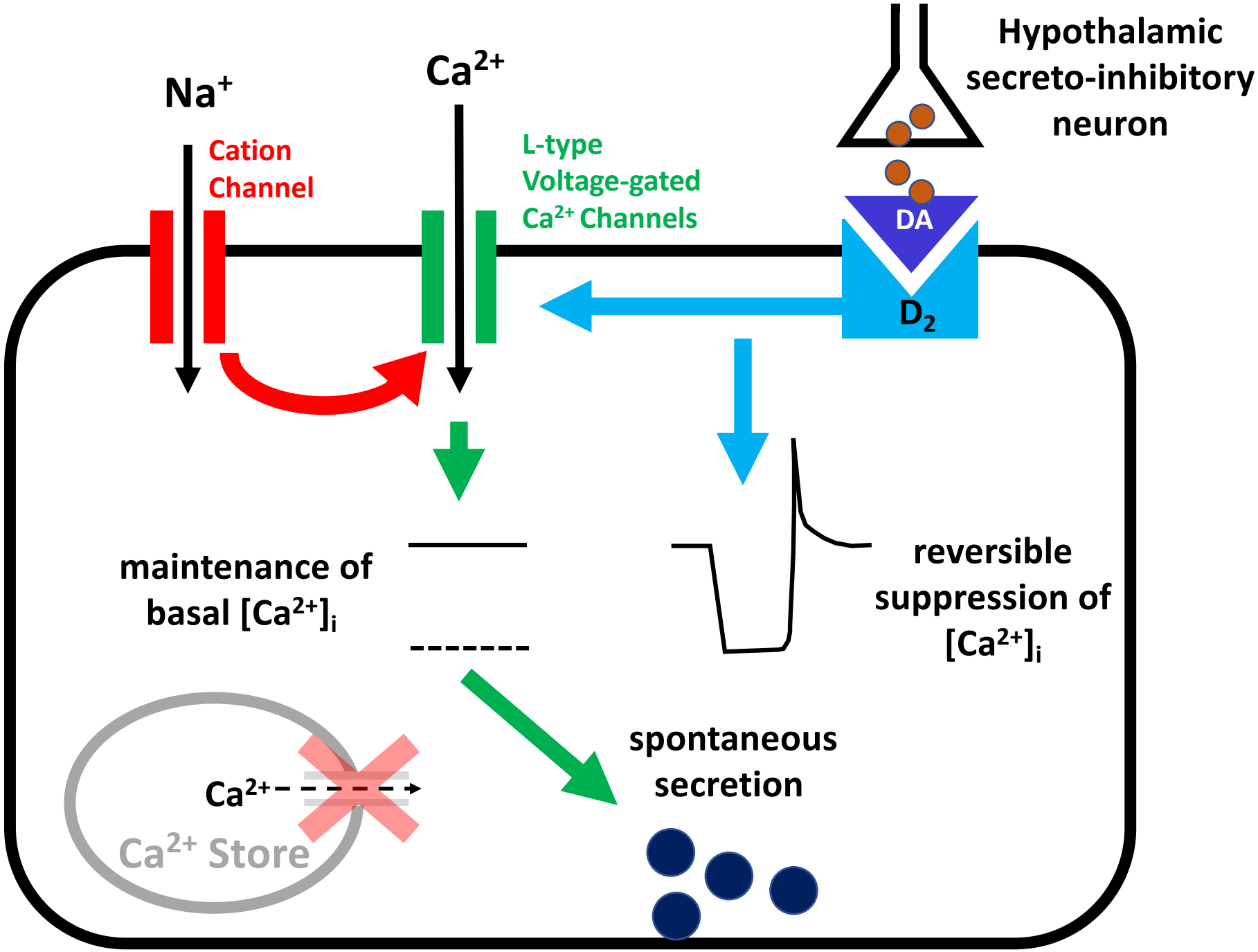

Pituitary melanotroph